Acta Cryst. (1997). B53, 466–475

The Deformation of Di-μ-halide Dinuclear Five-Coordinate Copper(II) Complexes in the Crystalline State

M. Bukowska-Strzyżewska, W. Maniukiewicz and L. Sieroń

Institute of General and Ecological Chemistry, Technical University, 90-924 Łódź, Poland

(*Received 26 July 1994; accepted 29 January 1997*)

Abstract

The coordination geometries of 154 dinuclear di-μ-chloro, di-μ-bromo and di-μ-fluoro five-coordinate (4 + 1) copper(II) complexes have been analyzed by the structural correlation method. Two reference Cu^{II} polyhedra have been established: (i) a trigonal bipyramid (TBP) in which the equatorial bond lengths are equal, but with the symmetry at the metal often deformed from D_{3h} to C_2, and (ii) an elongated square pyramid (SQP), with either a pyramidally or tetrahedrally distorted base, in which the *trans* valence angles are equal. Six different paths for the SQP⇌TBP deformation of the Cu^{II} coordination have been established from three criteria: (*a*) the location of the bridging ligands (axial and equatorial or equatorial and equatorial in TBP); (*b*) the nature of the deformation of the SQP base plane (pyramidal or tetrahedral); (*c*) whether a bridging or nonbridging bond is elongated in a SQP. The causes of the angular distortions from C_2 symmetry along the apical bond of a SQP, typical for the TBP⇌SQP Berry path, are analyzed. A progressive reduction of the tetragonal elongation of the Cu—*D* apical (SQP) bond length along the SQP⇌TBP transformation path and trigonal equalization of the three equatorial Cu—*D* (TBP) bonds are observed. The dependence of the average Cu—Cu′ distance and Cu—*X*—Cu′ angles on the deformation path are also established.

1. Introduction

The determination of the three-dimensional structure of a molecule by X-ray diffraction does not provide direct knowledge of its dynamic behavior. However, the fast progress of structural research has allowed Bürgi and Dunitz (Bürgi, 1973; Dunitz, 1979; Bürgi & Dunitz, 1994) to develop the *structural correlation* method, which allows the dynamic properties of molecules to be inferred from the correlated distributions of the deformations displayed by a given structural unit observed in many different crystal structures. The aim of the present work was to determine the paths of deformation of the Cu^{II} polyhedra in the complexes investigated and to analyze the deformations of the central Cu_2X_2 ring and of the Cu^{II} bond lengths and angles. The magnetic properties of di-μ-halide Cu^{II} complexes are known to be correlated with their bridge structure (Marsh, Patel, Hatfield & Hodgson, 1983; Nepven, Bormuth & Waltz, 1986; Blanchette & Willett, 1988; Bond, Willett & Rubenacker, 1990). Furthermore, the stereochemistry of penta-coordination continues to attract the attention of many investigators because of the great lability characteristic of complexes of this type and their role in many important chemical and biochemical processes (Holmes, 1984). The new dinuclear Cu^{II} complexes recently investigated by us showed considerable deformations from typical coordination geometry and, in some cases, unusual types of bridge (Bukowska-Strzyżewska & Maniukiewicz, 1992; Tosik *et al.*, 1991; Maniukiewicz & Bukowska-Strzyżewska, 1994; Tosik & Bukowska-Strzyżewska, 1994; Maniukiewicz, 1993).

2. Data retrieval

Dinuclear five-coordinate di-μ-halide Cu^{II} complexes were retrieved from the Cambridge Structural Database (1995; Allen *et al.*, 1979; Allen, Kennard & Taylor, 1983). The coordination numbers of both Cu^{II} atoms were required to be either exactly five or 4 + 1 with one bond distinctly (up to 50%) longer than the remainder. If Cu^{II} atoms occurred with different coordination numbers in the same dinuclear complex, the entry was rejected from the data set. Selections in terms of donor-atom types were achieved by the retrieval of appropriate subsets using the atom specification command in *QUEST*. The fragments analyzed were defined as

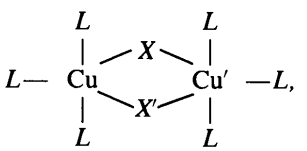

where L = Cl, Br, F, O, N or S and X = Cl, Br or F atoms. Structures with $R > 0.08$ were excluded. The detailed structural data of fragments considered and

the refcodes and literature citations have been deposited as supplementary material.*

3. The normalization of Cu^{II} bond lengths

To observe how bond lengths change with polyhedral deformation, the observed Cu—D bond lengths have been normalized to the average terminal, so that their mean values are equal to that for terminal Cu—Cl bonds not elongated by tetragonal elongation of a SQP. The average value obtained by us for a Cu—Cl_t bond length (from 113 individual values) is 2.259 Å, which is distinctly less than that of 2.323 Å given by Orpen, Brammer, Allen, Kennard & Watson (1989) for the Cu—Cl terminal bond in five-coordinate Cu^{II} complexes. The correction parameters we define as $\Delta r(D) = d_{av}(Cl_t) - d_{av}(D) = 2.259 - d_{av}(D)$, where $d_{av}(D)$ is the average value of the Cu—D bond lengths not elongated by tetragonal elongation of a SQP. The normalized bond lengths are then defined as $d^*(D) = d(D) + \Delta r(D)$. The correction parameters $\Delta r(D)$ for $D = Cl_{b,p}$, Br_t, $Br_{b,p}$, F_b, N, O and S are −0.040, −0.143, −0.187, +0.357, +0.261, +0.291 and −0.079 Å from 262, 25, 52, 5, 185, 79 and 15 averaged bonds, respectively. The b, p and t subscripts indicate, respectively, bridge bond in dinuclear fragments, bridge bonds in a polymeric structure and terminal bonds.

Normalization of the observed bond lengths using literature atomic radii cannot correct the elongated μ-Cu—X bonds. Where applicable, it gives results little different from ours. For Br, N, O and S atoms, for example, Pauling's atomic radii yield $\Delta r(D)$ values of −0.14 (−0.143), 0.29 (0.261), 0.33 (0.291) and −0.05 (−0.079) Å, where, for comparison, our corrections are given in parentheses.

4. The reference SQP and TBP polyhedra on the TBP⇌SQP paths and definition of individual deformation paths

The symmetrical coordination polyhedra of five-coordinate complexes are trigonal bipyramidal (TBP of D_{3h} symmetry) and square pyramidal (SQP of C_{4v} symmetry). It is convenient to assume for SQP coordination the central atom is displaced from the plane of the four basal atoms towards the apical position (Fig. 1). Because of this the *trans* valence angles of the SQP base, θ_{15}(SQP) and θ_{24}(SQP), are smaller than 180° and apical base valence angles are greater than 90°. Complexes of copper(II) exhibit a wide variety of irregular stereochemistries as a result of the lack of spherical symmetry of this d^9 ion. For five-coordinate Cu^{II} complexes, the five Cu—D bond lengths are usually not identical. Tetragonal elongation of the apical bond in SQP (4 + 1 geometry) and less pronounced trigonal compression of the axial bonds in TBP coordination are often observed (Addison, Nageswara Rao, Reedijk, van Rijn & Verschoor, 1984; Rossi & Hoffmann, 1974). Also observed are folded, or tetrahedrally distorted, elongated SQP geometries with C_2 symmetry and two *trans* apical base valence angles greater than and two less than 90°. Moreover, nondeformed SQP and TBP geometries of C_{4v} or D_{3h} symmetries are reported rather rarely. According to the Berry mechanism of intramolecular exchange of ligands in five-coordinate complexes (Berry, 1960), simultaneous angular deformation of two valence angles, θ_{15} and θ_{24}, leads to reversible transformation between SQP and TBP coordination with preservation of C_2 symmetry (Fig. 1).

Our analysis of the collected data (see below) shows that reference SQP and TBP polyhedra on the observed SQP⇌TBP paths of deformations may be determined as trigonal bipyramid (TBP), with equal equatorial bond lengths and angles often deformed from C_2 symmetry, and elongated square pyramid (SQP), with either a pyramidally or tetrahedrally distorted base and equalized *trans* valence angles. Some constraints on the TBP valence angles are required for the formation of four-membered Cu_2X_2 rings. The intra-ring X—Cu—X' valence angles are almost always near 90° and the equatorial position of both X bridge atoms indicates that only one equatorial TBP bond angle can be near 120°. To decide the tetrahedral or pyramidal deformation of the SQP base, two simultaneous requirements were considered: for pyramidal distortion $(\theta_{13} + \theta_{35}) > 180$° and $(\theta_{23} + \theta_{34}) > 180$°, while for tetrahedral distortion $(\theta_{13} + \theta_{35}) < 180$° and $(\theta_{23} + \theta_{34}) > 180$°.

To analyze the causes of the observed angular distortions retaining C_2 symmetry along the apical bond of SQP, typical for Berry pseudorotation, we propose six different paths of deformation (Fig. 2). They correspond to different modes of the incorporation of the individual five-coordinate Cu^{II} polyhedra in the dinuclear complexes and are based on three criteria: (*a*) whether the halide bridges are axial and equatorial or equatorial and equatorial in TBP, (*b*) whether SQP base

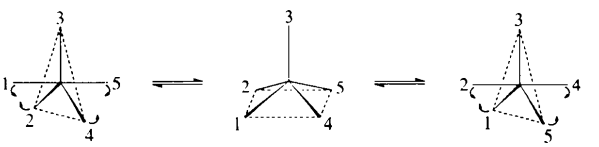

TBP (D_{3h}) θ_{15} = 180° θ_{24} = 120°

SQP (C_{4v}) $\theta_{15} = \theta_{24} < 180$°

TBP (D_{3h}) θ_{15} = 120° θ_{24} = 180°

Fig. 1. Berry deformation paths of five-coordinate complexes.

*Lists of bond angles, valence and torsion angles, trigonality parameters, deformation path data and refcodes have been deposited with the IUCr (Reference: MU0319). Copies may be obtained through The Managing Editor, International Union of Crystallography, 5 Abbey Square, Chester CH1 2HU, England.

plane is pyramidally or tetrahedrally deformed and (*c*) the elongated bond in a SQP is or is not incorporated in a $(\mu - X)Cu_2$ bridge.

The numerical values of the valence angles given in Fig. 2 are given from the least-squares lines (Fig. 3, Table 1), whose derivation is described below.

5. Analysis of TBP⇌SQP deformation paths

The analysis is based on the normalized Cu—*D* bond lengths and observed bond angles, θ_{ij}. The description of the polyhedral deformations by dihedral angles (Muetterties & Guggenberger, 1974; Holmes & Deiters, 1977) was not suitable because these methods assume equal Cu—*D* distances. These distances are not equal in the complexes analyzed, because different types of ligands are present. Tetragonal elongation of SQP polyhedra is evident sometimes and because of differences between μ and terminal Cu—*X* bonds.

In 1984, Addison and co-workers (Addison, Nageswara Rao, Reedijk, van Rijn & Verschoor, 1984) proposed a simple geometric parameter, defined as $\tau = (\theta_{15} - \theta_{24})/60$, as an index of the degree of trigonality in five-coordinate structures, within the structural continuum between TBP and SQP. For TBP $\tau = 1$ and for SQP coordination $\tau = 0$. The deformation of a five-coordinate polyhedron proceeds along the TBP⇌SQP Berry path if: (*a*) there is a synchronous change of the θ_{15} and θ_{24} angles from their values of 180 and 120° in a TBP to equality in a SQP and (*b*) the apical bond of the SQP remains an axis of C_2 symmetry during the transformation.

Fig. 3(*a*) gives the least-square line plots of θ_{15} *versus* τ and θ_{24} *versus* τ in the proposed six individual

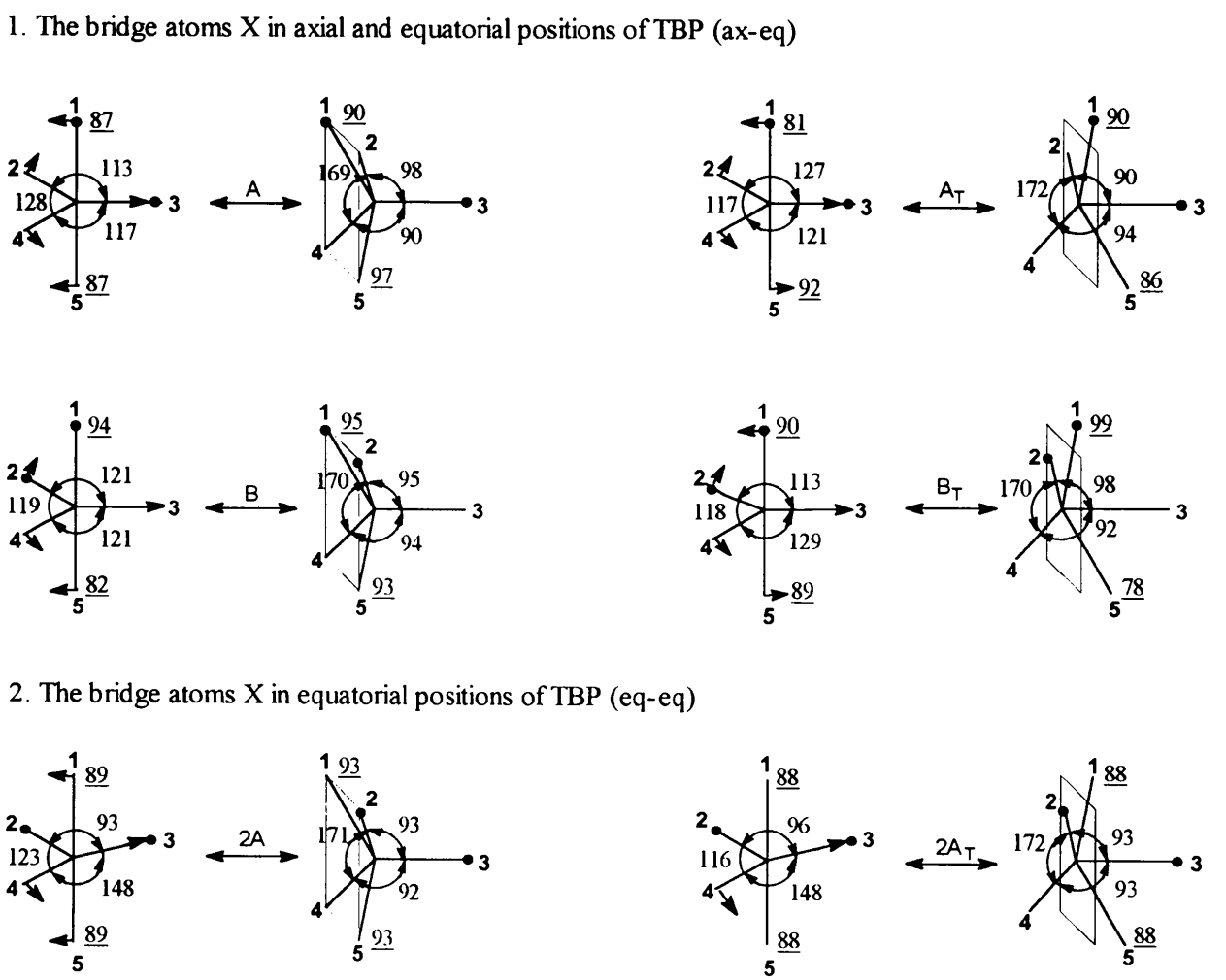

Fig. 2. The main deformation modes of CuX_2L_3 chromophores in the analyzed fragments. In analyzed CuX_2L_3 chromophores, the two largest valence angles are defined as θ_{15} and θ_{24}, fixing position 3 as the apical position of SQP. The numerical values of angles (°) are from the least-squares lines described in Table 1, θ_{13} and θ_{35} angles are underlined. •: The bridging *X* atom. *A*, 2*A*, *B*: SQP with pyramidal distortion of the base plane. A_T, $2A_T$, B_T: SQP with tetrahedral distortion of the base plane.

Table 1. *The expected values of y functions for SQP and TBP coordination based on least-squares lines and their correlation parameters*

The average deviations of the observed y values from the lines are from 2 to 3° for $y_{1\text{-}3}$ lines, from 4 to 7° for $y_{4\text{-}8}$ lines, from 0.04 to 0.12 Å for y_9 and y_{11} lines and from 0.01 to 0.04 Å for y_{10} lines.

Path	A	B	$2A$	A_T	B_T	$2A_T$
			$y_1 = \theta_{15} = m\tau + b$			
y_1 (SQP) $= b$	169.0	170.1	171.4	170.9	170.1	171.8
y_1 (TBP) $= m + b$	187.6	178.9	183.1	176.7	178.3	176.1
r	0.708	0.351	0.482	0.230	0.439	0.235
			$y_2 = \theta_{24} = m\tau + b$			
y_2 (SQP) $= b$	169.0	170.1	171.4	171.8	170.4	171.8
y_2 (TBP) $= m + b$	127.7	119.0	123.2	116.9	118.3	116.2
r	−0.910	−0.904	−0.917	−0.911	−0.956	−0.952
			$y_3 = \theta_{23} + \theta_{34} = m\tau + b$			
y_3 (SQP) $= b$	188.0	189.2	185.2	183.9	189.4	186.0
y_3 (TBP)$= m + b$	230.2	241.9	241.1	248.4	241.4	244.5
r	0.764	0.883	0.928	0.907	0.954	0.955
			$y_4 = \theta_{23} = m\tau + b$			
y_4 (SQP) $= b$	98.2	95.1	92.9	89.9	97.6	92.8
y_4 (TBP) $= m + b$	113.2	121.4	93.3	127.1	112.7	96.2
r	0.280	0.659	0.025	0.554	0.341	0.190
			$y_5 = \theta_{34} = m\tau + b$			
y_5 (SQP) $= b$	89.8	94.1	92.3	94.0	91.8	93.2
y_5 (TBP) $= m + b$	117.1	120.5	147.8	121.3	128.7	148.3
r	0.528	0.607	0.906	0.430	0.714	0.898
			$y_6 = \theta_{13} + \theta_{35} = m\tau + b$			
y_6 (SQP) $= b$	187.2	188.9	186.0	176.6	176.4	174.9
y_6 (TBP) $= m + b$	173.9	176.3	178.8	173.0	178.6	176.4
r	−0.536	−0.374	−0.379	−0.126	0.212	0.071
			$y_7 = \theta_{13} = m\tau + b$			
y_7 (SQP) $= b$	90.0	95.5	93.0	90.2	98.9	87.6
y_7 (TBP) $= m + b$	87.2	94.4	89.4	81.0	89.9	88.1
r	−0.105	−0.032	−0.129	−0.428	−0.332	0.029
			$y_8 = \theta_{35} = m\tau + b$			
y_8 (SQP) $= b$	97.2	93.4	93.0	86.4	77.5	87.6
y_8 (TBP) $= m + b$	86.7	81.9	89.4	92.0	88.8	88.1
r	−0.339	−0.307	−0.129	0.197	0.407	0.029
			$y_9 = d_3^* = m\tau + b$			
y_9 (SQP) $= b$	2.759	2.674	2.738	2.869	2.700	2.937
y_9 (TBP) $= m + b$	2.328	2.355	2.279	2.345	2.402	2.331
r	−0.482	−0.352	−0.657	−0.636	−0.497	−0.777
			$y_{10} = (d_2^* + d_4^*)/2 = m\tau + b$			
y_{10} (SQP) $= b$	2.249	2.247	2.226	2.257	2.257	2.157
y_{10} (TBP) $= m + b$	2.323	2.353	2.455	2.297	2.305	2.448
r	0.455	0.613	0.677	0.268	0.259	0.931
			$y_{11} = d_3^* - (d_2^* + d_4^*)/2 = m\tau + b$			
y_{11} (SQP) $= b$	0.510	0.426	0.511	0.612	0.443	0.390
y_{11} (TBP) $= m + b$	0.005	0.001	−0.176	0.048	0.097	−0.059
r	−0.524	−0.444	−0.706	−0.657	−0.452	−0.878

On the paths $2A$ and $2A_T$ θ_{13} and θ_{35} are not distinguishable and $y_7 = y_8 = (\theta_{13} + \theta_{35})/2$.

paths of deformation. The extrapolated values for SQP ($\tau = 0$) and TBP ($\tau = 1$) derived from these lines are given in Table 1. For the six paths, the point at $\tau = 0$ where θ_{15}(SQP) $= \theta_{24}$(SQP) ranges only from 169.0° on the A path to 171.8° on the $2A_T$ path. The extrapolated values of θ_{24}(TBP) and θ_{15}(TBP) are near those for the ideal TBP of 120 and 180° (they range from 116.2 and 176.1° on the $2A_T$ path to 127.7 and 187.6°, respectively, on path A). The observed differences θ_{15}(TBP) − θ_{24}(TBP) are almost exactly 60° (from 59.1 to 60.1°). The plots of θ_{15} *versus* τ for the A_T, B_T and $2A_T$ paths slope less than those for the A, B and $2A$ paths (the average gradient, m_{av}, is 6.0° in the first case and −13.0° in the second). In contrast, the plots of θ_{24} *versus* τ slope more in the first case ($m_{av} = -53.9$°) than in the second (m_{av} for A, B and $2A$ paths is −46.2°). In general, for all paths of deformation synchronized change of θ_{15} and θ_{24} is

observed, with $\theta_{15} = \theta_{24}$ for $\tau = 0$ and $\theta_{15} - \theta_{24} = 60°$ for $\tau = 1$.

The least-squares lines $y_3 = (\theta_{23} + \theta_{34})$ *versus* τ and $y_4 = (\theta_{13} + \theta_{35})$ *versus* τ are shown in Fig. 3(*b*). The values $(\theta_{23} + \theta_{24})$ for $\tau = 0$ on the paths A, B and $2A$ are equal to the values $(\theta_{15} + \theta_{35})$ for $\tau = 0$ and the sums $(\theta_{23} + \theta_{34}) + \theta_{24}$ and $(\theta_{13} + \theta_{35}) + \theta_{15}$ are near 360° (from 357 to 360°), indicating the coplanarity of two sets of four atoms: Cu, D_2, D_4, D_3 and Cu, D_1, D_5, D_3. On the paths A_T, B_T and $2A_T$, because $\theta_{15} \leq \pi$, the coplanarity of the Cu, D_1, D_5 and D_3 atoms requires that $\theta_{15} = (\theta_{13} + \theta_{35})$. The observed differences (from 3 to 6°) are greater than for the paths with a pyramidally deformed SQP base. The values of $(\theta_{23} + \theta_{34})$ and $(\theta_{13} + \theta_{35})$ for $\tau = 1$ (see Table 1) are near to those expected for a TBP, 240 and 180°, and indicate the coplanarity of the three Cu—D_2, Cu—D_3, Cu—D_4 and three Cu—D_1, Cu—D_3, Cu—D_5 bonds on SQP⇌TBP paths.

In the fragments analyzed, C_2 symmetry, which requires that $\theta_{23} = \theta_{34}$ and $\theta_{13} = \theta_{35}$, is often destroyed. As we can see from Fig. 2, the largest angular deformation from C_2 symmetry is observed on the paths $2A$ and $2A_T$ for the coordination polyhedra near to TBP. The observed $(\theta_{34} - \theta_{23})$ differences, which vary from 55° for TBP to 1° for SQP on these paths, are caused by the limitation of the (equatorial in TBP) intra-Cu_2X_2 ring X—Cu—X' angle to *ca* 93–96°. To observe the possible influence of different sizes of the ligand donor atoms on the deformation of the valence angles, the polyhedra have been divided into four types: CuX_5, CuX_4L, CuX_3L_2 and CuX_2L_3, where X and L atoms have distinctly different sizes. Table 2 gives the distribution of these types of chromophores over the established deformation paths and indicates explicitly any angular distortions from C_2 symmetry, defined as $\Delta_1 = |\theta_{23} - \theta_{34}|$ and $\Delta_2 = |\theta_{13} - \theta_{35}|$, which are greater than 20°. The largest distortions are displayed by Δ_1. In 31 strongly deformed mainly CuX_3L_2 and CuX_5 polyhedra $\Delta_1 > 20°$ is observed 26 times and Δ_2 only five times. On the A and A_T paths in CuX_3L_2 polyhedra, where the two bridging X atoms occupy the positions 1 and 3 and the third large atom position 2, it is always true that $\theta_{23} > \theta_{34}$. For CuX_3L_2 polyhedra, the average

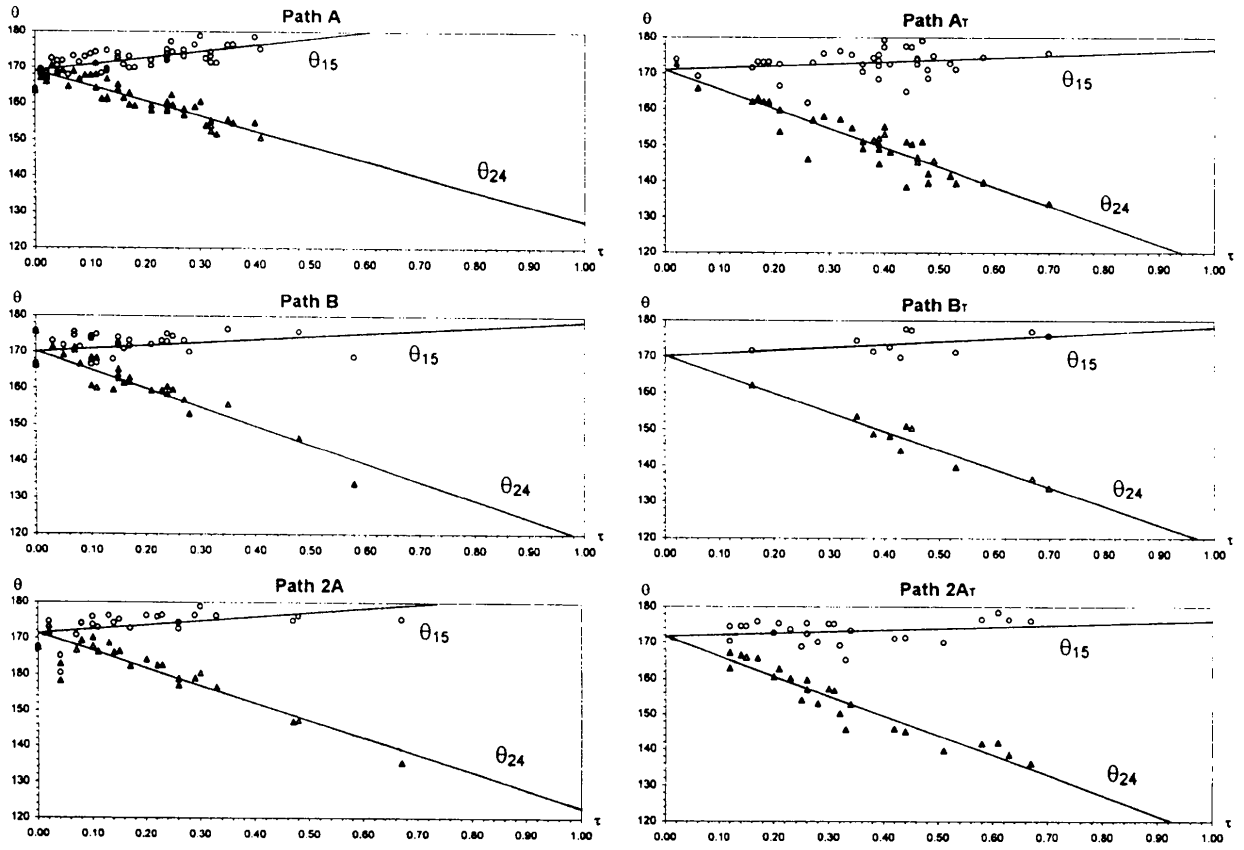

(*a*)

Fig. 3. The least-squares lines on the six paths of deformation. (*a*) The valence angles θ_{15} and θ_{24} *versus* τ. (*b*) The sums of angles $(\theta_{23} + \theta_{24})$ and $(\theta_{13} + \theta_{35})$ *versus* τ. (*c*) The normalized tetragonally elongated bonds d_3^*, the average values $(d_2^* + d_4^*)/2$ and the differences $d_3^* - (d_2^* + d_4^*)/2$ *versus* τ.

value of $(\theta_{23} - \theta_{34})_{av} = 13°$, whereas for the remaining types of polyhedra $(\theta_{23} - \theta_{34})_{av} = -2°$. This indicates the distinct effect of different donor-atom sizes on the angular deformation of Cu^{II} polyhedra. On path A, where this type of polyhedron dominates and the deformation proceeds for the τ values from 0 to ~0.4, the influence of this deformation is visible as $\theta_{23} > \theta_{34}$ for SQP coordination. On the less occupied paths B and B_T, the deformation from C_2 symmetry of CuX_3L_2 polyhedra is often revealed by large values of Δ_2, because of the differing sizes of D_1 and D_2 atoms, not involved in the bridge formation, and the apical D_3 atom. The large deformation from C_2 symmetry of CuX_5 polyhedra is observed mainly on the path A_T. These deformations cannot be explained by the different sizes of coordinated atoms. In our opinion, they may be caused by the polymeric character of the structures analyzed or by interionic N(O)—H···X hydrogen bonds.

Fig. 3(*c*) displays the variation of the normalized tetragonally elongated bond lengths, d_3^*, the average values of equatorial TBP distances, $(d_2^* + d_4^*)/2$, and the differences $d_3^* - (d_2^* + d_4^*)/2$ with τ for the different deformation paths SQP⇌TBP. Linear correlation of these values with τ is observed. The extrapolated values for ideal SQP and TBP are given in Table 1. The tetragonal elongation of the $d_3{}^*$ bond is a distinct effect. The average d_3^*(SQP) values vary from 2.937 Å on $2A_T$ to 2.674 Å on the B path. The average d_3^*(TBP) values range from 2.402 (B_T) to 2.279 Å ($2A$). The three equatorial Cu—$D_{2,3,4}$(TBP) bonds are mostly equal on the paths A, B and A_T, with respective average values of 2.325, 2.354 and 2.321 Å. On paths $2A$ and $2A_T$ (contrasting with path B_T) the d_3^*(TBP) bond is a little shorter than the average value of $(d_2^* + d_4^*)/2$ (TBP). Fig. 3(*c*) shows that the trigonal equalization of the three equatorial bonds in TBP (d_2, d_4 and d_3) is observed to different degrees for the analyzed paths of deformation. The tetragonal elongation of the apical d_3^* bond is illustrated by the plot of the least-squares line of $d_3^* - (d_2^* + d_4^*)/2$ *versus* τ. This elongation for reference SQP polyhedra is from 0.390 to 0.612 Å on the $2A_T$ and A_T paths, respectively, but near 0° for TBP coordination. The shortening of the axial TBP bonds, d_1^* and d_5^*, was not observed for any deformation paths. The least-squares line for all average $(d_1^* + d_5^*)/2$ values *versus* τ is strictly parallel to the τ axis, and indicates a constant value for $(d_1^* + d_5^*)/2$ of 2.253 Å, the average displace-

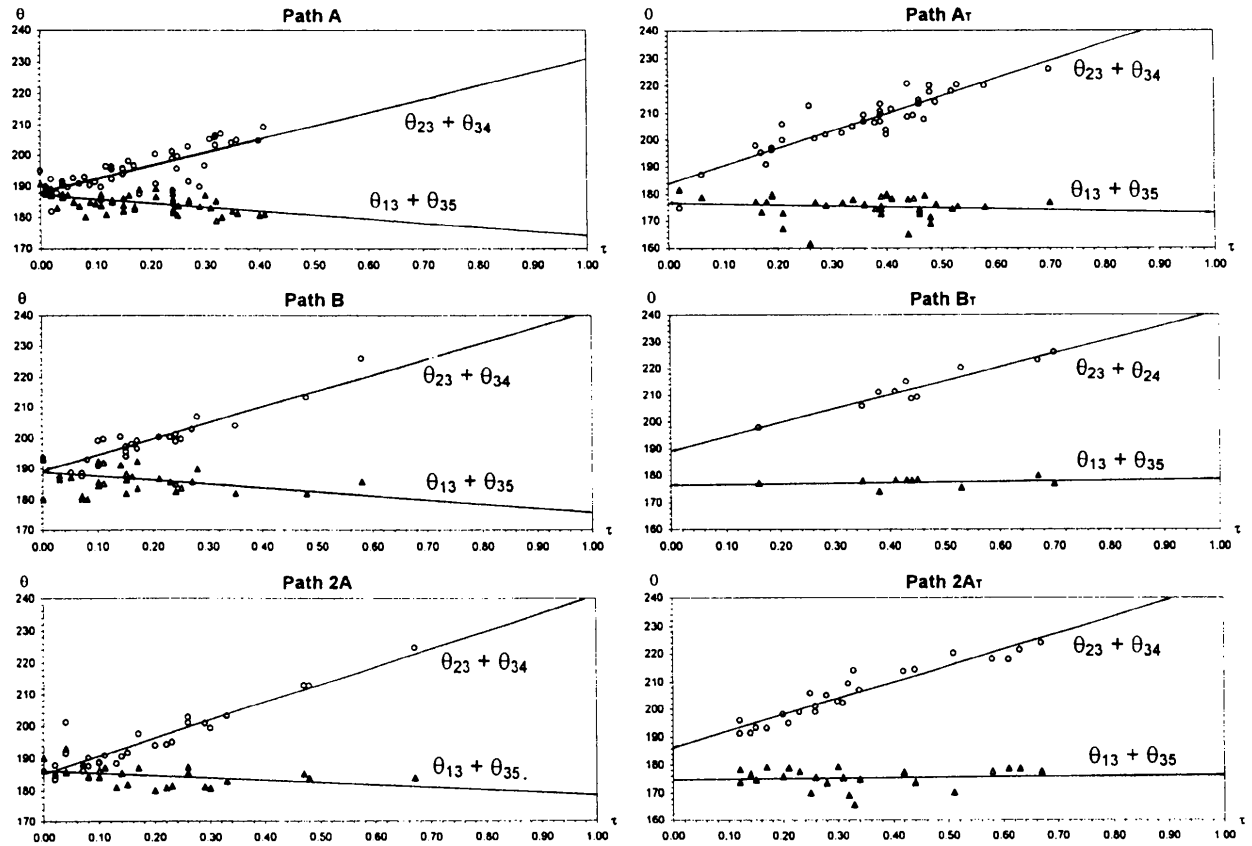

(*b*)

Fig. 3 (*cont.*)

ment of the experimental points from the line is 0.023 Å.

To recapitulate: TBP⇌SQP paths of deformation proceed from a TBP, with three equal equatorial bond lengths, more or less deformed from C_2 symmetry, to a SQP with four slightly shortened basal bonds, a distinctly elongated apical bond and often deviation less from C_2 symmetry than the corresponding TBP.

As we can see from Fig. 2, the A path proceeds between a TBP with almost ideal C_2 symmetry and a SQP more deformed from C_2 symmetry. The unsynchronized reduction of the θ_{23} and θ_{34} equatorial angles ($\theta_{23} > \theta_{35}$ in SQP) may be explained by the influence of the third large atom X in position 2 in the majority of deformed CuX_3L_2 polyhedra belonging to this path. Unsynchronized increase of θ_{13} and θ_{35} angles ($\theta_{35} > \theta_{15}$ in SQP) may be caused by the limitation of the θ_{13} angle to ~90° in the four-membered Cu_2X_2 ring.

The A_T path proceeds between a less symmetrical TBP and a more symmetrical SQP by the asymmetric change of θ_{13} and θ_{35} angles. The first distinctly increases, the second is reduced. The reduction of the equatorial θ_{23} and θ_{34} angles is also not fully symmetrical.

The B path proceeds between a slightly asymmetric TBP (the axial angles $\theta_{13} > \theta_{35}$ are asymmetrically involved in the bridge formation) and a practically symmetrical SQP by simultaneous reduction of the equatorial θ_{23} and θ_{34} angles.

The B_T path proceeds asymmetrically between asymmetrical polyhedra, but the small sample size (only 10 polyhedra) makes detailed analysis pointless.

The $2A$ and $2A_T$ paths are unsymmetrical, proceeding between a TBP which is not symmetrical in the equatorial plane and a symmetrical SQP. In the equatorial plane of the TBP, only one θ_{34} angle is reduced. On the $2A_T$ path the θ_{13} and θ_{35} angles are nearly constant.

6. The deformation of the central Cu_2X_2 ring

The chemical formulae of the fragments analyzed, excluding two we recently investigated (Tosik *et al.*, 1991; Tosik & Bukowska-Strzyżewska, 1994), are symmetrical. Symmetrical linking of the Cu and Cu′

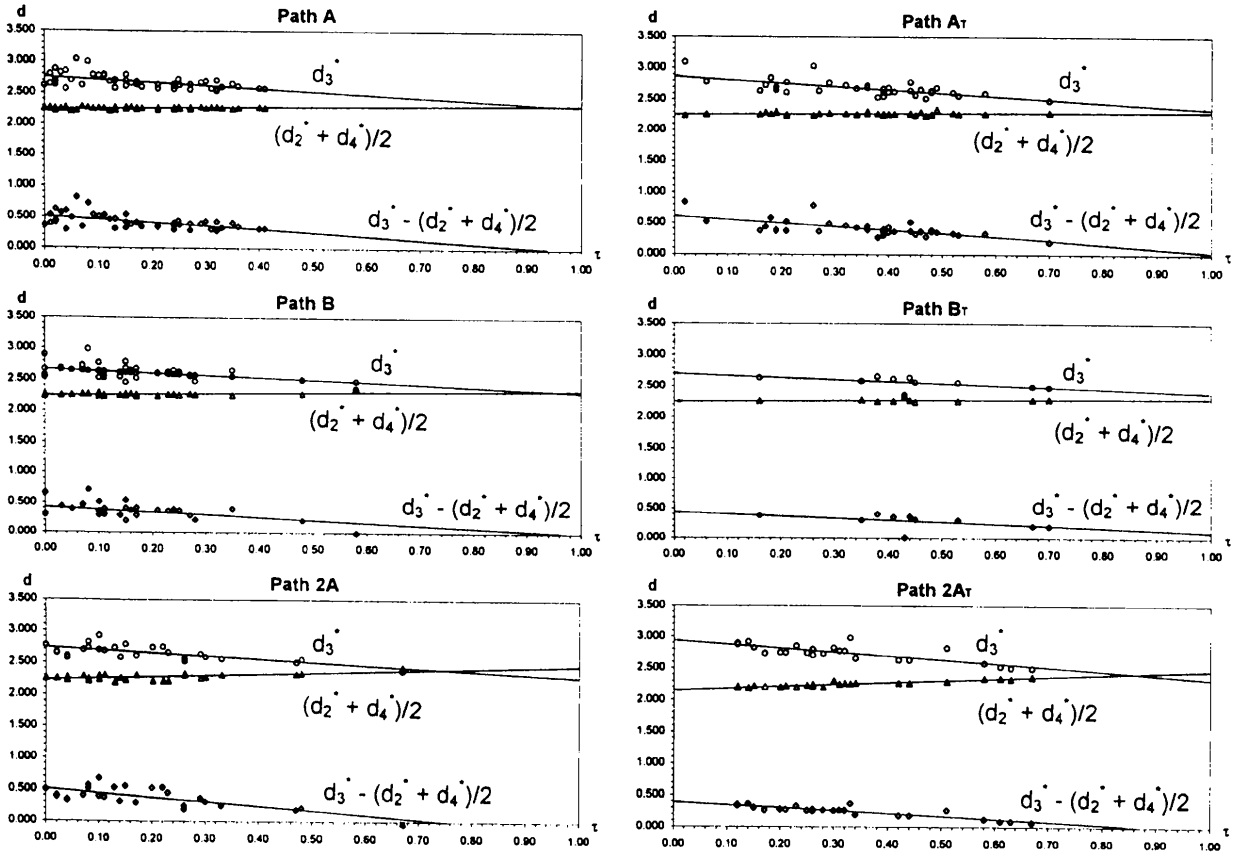

(*c*)

Fig. 3 (*cont.*)

Table 2. *The distribution of individual types of chromophore on individual paths of deformation and specification of distortions greater than 20° from C_2 symmetry along the apical bonds of SQP defined as: $\Delta_1 = |\theta_{23} - \theta_{34}|$ and $\Delta_2 = |\theta_{13} - \theta_{35}|$*

Path of deformations	No. of chromophores (in all)	No. of chromophores	Refcode	Δ_1	Δ_2	No. of chromophores	Refcode	Δ_1	Δ_2
		CuX_5L				CuX_4L			
A	51	14	PIBPEV		21.2	2			
A_T	38	19	DARGUY	21.0		3	BARTOD	32.9	
			DARHAF	20.6					
			ENNCCUC10	22.0					
			FIRWIMO1	22.5					
			TABNOZ	20.9					
			MPEATC10	22.8					
$2A$	26	-				-			
$2A_T$	24	-				-			
B	35	30	TABNOZ	33.3		3			
B_T	10	8	TABNOZ	20.8		-			
			MPEATC10	22.8					
In all	184	71				8			
		CuX_3L_2				CuX_2L_3			
A	51	28	CIKJIP	23.8	23.4	7			
			FAGXEQ	36.9					
			FAGXOA	26.9					
			GALBUQ	28.5					
			HAHNEJ	26.0					
A_T	38	13	MEPCUB10	26.4		3			
			PIMPEG	45.7					
$2A$	26	15	FAGXOA		23.6	11	JONKOM	22.6	
			JITDAR	44.3					
$2A_T$	24	10	BIPVEB	25.7		14	HEJWOI	23.2	
			BIPVEB	36.5					
			FACJUO	32.4					
			HEJWIC	29.0					
			JONKOM	30.5					
			TMSCCU	31.3					
			YENDOK	29.9					
B	35	1	SOCWUC		35.4	1			
B_T	10	2	ESALCU 10		31.3				
In all	184	69				36			

polyhedra is observed only in 80% of fragments analyzed (in 76% the correction is by a symmetry center, in 4% by a C_2 axis). The departure of the Cu—X—X'—Cu torsion angles from 180° indicates the non-planarity of this ring in 24% of fragments. The observed deviations from 180° vary from 0.5 to 56.5°, with a mean of 22.7°. Average Cu—Cu′ distances and Cu—X—Cu′ bridge angles are given in Table 3. In the majority of the Cu_2X_2 rings both Cu^{II} polyhedra are deformed along the same type of deformation path: A/A or A_T/A_T paths occur in 74 fragments, B/B or B_T/B_T in 35 fragments and $2A/2A$ or $2A_T/2A_T$ in 36 fragments; only nine fragments contain Cu^{II} polyhedra with different localization of bridges: five of these contain one Cu^{II} polyhedron deformed along A or A_T path and a second along a $2A$ or a $2A_T$ path, while in four fragments one Cu chromophore is deformed along B and a second along an A or A_T path. As can be expected, the average values of Cu—Cu′ distances for all path deformations (with the exception of one asymmetrical strongly nonplanar Cu_2Br_2 ring) increase with the size of the X atom. The observed elongation of Cu—Cu′ distances is here correlated with a small reduction of the average Cu—X—Cu′ bridge angles (except for the $2A_T/2A_T$ path, where the three Cu_2Br_2 rings available are insufficient for statistical analysis). For complexes with axial–equatorial bridges, distinctly longer Cu—Cu′ distances and smaller Cu—X—Cu′ angles are observed on the paths A/A and A_T/A_T than on the paths B/B and B_T/B_T. This is connected with the lack of the tetrahedral elongation of the bridge bonds on the latter paths. The smallest Cu—X—Cu′ intra-ring angles are observed on the paths $2A/2A$ and $2A_T/2A_T$, with both bridges equatorial. This is connected with distinctly larger X—Cu—X' intra-ring valence angles.

A unique form of the Cu_2X_2 ring is observed in the two structures mentioned above, which have different sets of donor atoms at the Cu and Cu′ centers. These structures show a large degree of trigonality of the Cu coordination polyhedra (τ from 0.47 to 0.67), equatorial–equatorial localization of the bridges and a planar central Cu_2X_2 ring with one bridging X atom forming

Table 3. *Statistical data for Cu_2X_2 rings on individual paths of Cu/Cu′ polyhedra deformation*

The data are given in order: no. of fragments, Cu—Cu′ average distance (Å), Cu—X—Cu′ average bridge angle (°).

Scheme of Cu_2X_2 ring		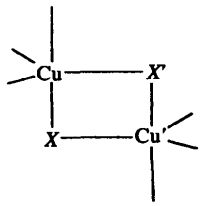			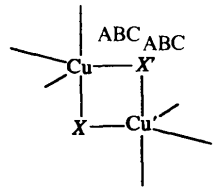			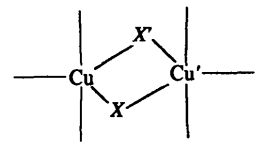			Axial–equatorial/ equatorial–equatorial bridges	Axial–equatorial bridge
X	Path	A/A	A/A_T	A_T/A_T	B/B	B/B_T	B_T/B_T	$2A/2A$	$2A/2A_T$	$2A_T/2A_T$	$A(A_T)/2A(2A_T)$	$A(A_T)/B$
		1		4								
F		3.137	–	3.009	–	–	–	–	–	–	–	–
		98.0		94.2								
		31	2	23	20	1	9	13	5	12	4	4
Cl		3.533	3.650	3.640	3.415	3.438	3.436	3.471	3.453	3.320	4.308	3.407
		89.9	91.3	92.9	94.8	96.2	95.5	87.1	85.5	81.1	84.9	92.0
		9		4	5			2	1	3	1	
Br		3.750	–	3.692	3.547	–	–	3.598	3.489	3.635	3.318	–
		90.0		88.6	92.9			85.4	82.9	84.3	79.3	

two tetragonally elongated bonds and the second two undistorted bonds. There is a large difference between the two Cu—X—Cu′ and Cu—X'—Cu′ bridge angles in each structure (81.8–89.1 and 80.2–85.6°). This mode of bridging has not previously been observed. We recently investigated complexes of the type

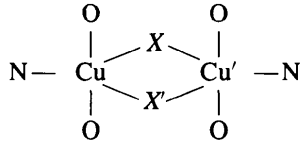

(Bukowska-Strzyżewska & Maniukiewicz, 1992; Maniukiewicz & Bukowska-Strzyżewska, 1994; Maniukiewicz, 1993), which exemplify symmetrical deformation by tridentate ligands which form chelate complexes with condensed six- and five-membered rings. The spatial constraints lead to distinct non-planarity of the central Cu_2Cl_2 rings, different degrees of trigonality of both Cu^{II} polyhedra and also unsymmetrical solvation.

7. Conclusions

The density of the points in Fig. 3 between $\tau = 0$ (SQP) and $\tau = 1$ (TBP) indicates easy deformation of SQP coordination in the range from $\tau = 0$ to $\tau = 0.4$ for SQP with pyramidally deformed bases and in the range $\tau = 0.1$ to $\tau = 0.6$ for SQP coordination with tetragonally deformed bases.

Structural distortion of Cu^{II} coordination polyhedra proceeds from an elongated square pyramid, with a pyramidally or tetrahedrally deformed base, towards a trigonal bipyramid, with simultaneous change of the basal θ_{15} and θ_{24} angles from ~170 to 180° and from ~170 to 120°, respectively, with a reduction in the tetragonal elongation of the apical SQP bond and trigonal equalization of the three equatorial TBP bond lengths to values a little longer than those for the basal bonds in SQP.

The angular constraints imposed by the four-membered Cu_2X_2 rings (and in special cases by the different sizes of the donor atoms) produce distinct angular deformations from the C_2 symmetry typical of the SQP⇌TBP Berry path. Most often a difference between the equatorial TBP θ_{23} and θ_{34} angles is observed. The deformation paths preserve the coplanarity of Cu—$D_3D_2D_4$ and Cu—$D_3D_1D_5$ units. The dependence of average Cu—Cu′ distances and Cu—X—Cu′ bridge angles on the positions of the bridge atoms and of the tetragonally elongated bonds, and on the nature of the X atoms has been established.

This work was supported by the Polish Scientific Research Committee (KBN) under grant 2 2644/92/03.

References

Addison, A. W., Nageswara Rao, T., Reedijk, J., van Rijn, J. & Verschoor, G. C. (1984). *J. Chem. Soc. Dalton Trans.* pp. 1349–1355.

Allen, F. H., Bellard, S., Brice, M. D., Cartwright, B. A., Doubleday, A., Higgs, H., Hummelink, T., Hummelink-Peters, B. G., Kennard, O., Motherwell, W. D. S., Rodgers, J. R. & Watson, D. G. (1979). *Acta Cryst.* B**35**, 2331–2339.

Allen, F. H., Kennard, O. & Taylor, R. (1983). *Acc. Chem. Res.* **16**, 146–153.

Berry, R. S. (1960). *J. Chem. Phys.* **32**, 933–938.

Blanchette, J. F. & Willett, R. D. (1988). *Inorg. Chem.* **27**, 843–849.

Bond, M. R., Willett, R. D. & Rubenacker, G. V. (1990). *Inorg. Chem.* **29**, 2713–2720.

Bukowska-Strzyżewska, M. & Maniukiewicz, W. (1992). *J. Cryst. Spectrosc. Res.* **22**, 43–49.

Bürgi, H.-B. (1973). *Inorg. Chem.* **12**, 2321–2325.

Bürgi, H.-B. & Dunitz, J. D. (1994). *Structure Correlation*. New York, Basel, Cambridge, Tokyo: Weinheim.

Cambridge Structural Database (1995). Version 5.10. Cambridge Crystallographic Data Centre, 12 Union Road, Cambridge, England.

Dunitz, J. D. (1979). *X-ray Analysis and the Structure of Organic Molecules*. Ithaca, London: Cornell University Press.

Holmes, R. R. (1984). *Prog. Inorg. Chem.* **32**, 119–235.

Holmes, R. R. & Deiters, J. A. (1977). *J. Am. Chem. Soc.* **99**, 3318–3326.

Maniukiewicz, W. (1993). Dissertation for the doctor's degree, Institute of General Chemistry, Łódź.

Maniukiewicz, W. & Bukowska-Strzyżewska, M. (1994). *J. Chem. Crystallogr.* **24**, 133–137.

Marsh, W. E., Patel, K. C., Hatfield, W. E. & Hodgson, D. J. (1983). *Inorg. Chem.* **22**, 511–515.

Muetterties, E. L. & Guggenberger, L. J. (1974). *J. Am. Chem. Soc.* **36**, 1748–1756.

Nepven, F., Bormuth, F. J. & Waltz, L. (1986). *J. Chem Soc. Dalton Trans.* pp. 1213–1216.

Orpen, A. G., Brammer, L., Allen, F. H., Kennard, O. & Watson, D. G. (1989). *J. Chem. Soc. Dalton Trans.* p. S1.

Rossi, A. R. & Hoffmann, R. (1974). *Inorg. Chem.* **14**, 365–373.

Tosik, A. & Bukowska-Strzyżewska, M. (1994). *J. Chem. Crystallogr.* **24**, 139–143.

Tosik, A., Maniukiewicz, W., Mroziński, J., Sigalas, M. P., Tsipis, C. A. & Bukowska-Strzyżewska, M. (1991). *Inorg. Chem. Acta*, **190**, 199–203.